

# Phys Enph 479/879 Assignment #5: FDTD and Maxwell's Equations

Michael Jafs<sup>1,\*</sup>

<sup>1</sup>*Department of Physics, Engineering Physics and Astronomy,  
Queen's University, Kingston, ON K7L 3N6, Canada*  
(Dated: April 17, 2022)

The finite-difference time-domain (FDTD) method is used to solve Maxwell's equations in one dimension (1D) and finally in 2D. We show our results of implementing absorbing boundary conditions and the results of our model successfully executing the full-field scattered-field approach. We add a linear dielectric thin film and analyze the transmission and reflection of a 2-fs pulse as it interacts with the thin film. We investigate the effects of sending a 1-fs pulse through a thin film being described by each a Drude and a Lorentz dispersion model. Finally, we consider a 2D FDTD case in which we model transverse magnetic modes and simulate the intensity of the electric field over time. We conclude by comparing run times from basic python "speed-up" techniques from the use of numba and vectorization, before parallelizing our code and running on CAC. We provide example plots of the 2D case on a large grid size and show how dividing the work over multiple processes, we can achieve a faster time per process, as expected.

## I. RESULTS

### A. ABC's and Linear Dielectric Implementation

Since our base FDTD code for calculating the electric field propagation in one dimension (1D), interacts with the boundary as if it is metallic as a default, we began by implementing a set of absorbing boundary conditions (ABC's) which serve to terminate the grid. Thus, we expect after implementation, for the electric field to freely pass through the walls of our simulation. We chose our grid spacing to have units of  $dx = 20 \text{ nm}$ , and calculated our time-step size based off of  $dx$ , so that  $dt = dx/2c$ , where  $c$  is the speed of light. Therefore, our simulation stepped forward in time, in steps of size  $dt = 3.33 \times 10^{-17} \text{ s}$ . Our set-up implies that our grid is vacuum so our pulse will travel at a speed  $c$ . Using a grid size of 801x801 grid points, we injected a 2 femto-second (fs) pulse at a location of 200 in units of grid points, and tracked its motion with a simple animation to view the ABC's. For a total run time of 2000 steps of  $dt$ , the results of the ABC's are shown in Fig. 1, for which it is clear that the pulse leaves the frame completely with no discernible reflection.

Next, we implemented the total-field scattered-field (TFSF) approach, since in the presence of a dielectric or another case resulting in a backwards scattered field, we wanted to be able to analyze the purely scattered field, without overlap from the initial source. Using the identical pulse and grid parameters as before the ABCs, we produced plots of the results following the TFSF implementation. From the view of the entire grid, there is zero backward injected field (2a), however, numerically we expect a small, but detectable backward injected field. The amount of field which is still injected backward following the TFSF approach is shown in Fig. 2d. We have nevertheless managed to reduce the backward injected field by a significant and sufficient margin.

With ABCs and the TFSF approach in place, we decided to model the effects of the injected pulse, interacting with

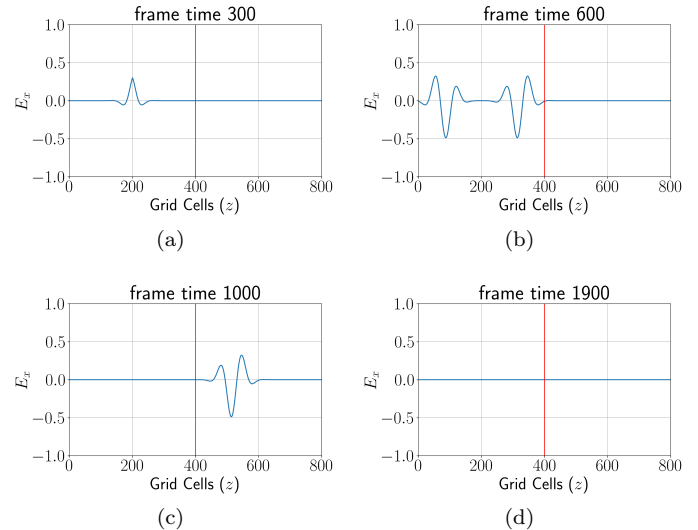


Figure 1. 2 fs pulse injected in 1D with absorbing boundary conditions. (a) - (d) show the pulse at sequential time-steps. Ran for a total time of 2000 time-steps.

a thin film possessing a non-zero dielectric constant. With our same grid, we modeled the interaction of our pulse from before, with a  $1\mu\text{m}$  thin film with dielectric constant  $\epsilon = 9$ . This is the same as setting the index of refraction  $n$  of the thin film equal to 3. It is of interest to consider the amount of electric field which manages to permeate the thin film and also the amount that gets reflected when it makes contact with the medium. For this, we calculated the transmission and reflection coefficients:

$$T = \left| \frac{E_t(\omega)}{E_{in}(\omega)} \right|^2, \quad R = \left| \frac{E_r(\omega)}{E_{in}(\omega)} \right|^2, \quad (1)$$

where  $E_t$  is the transmitted field and  $E_r$  is the reflected field.

In order to extract the information in the frequency domain, we had to wait until virtually no field was left in the frame. This amounted to waiting for roughly 4000 time-steps. Once again, we ran our simulation for a 2 fs pulse, for which we have shown the behaviour of the 1D electric field

\* 17msj2@queensu.ca

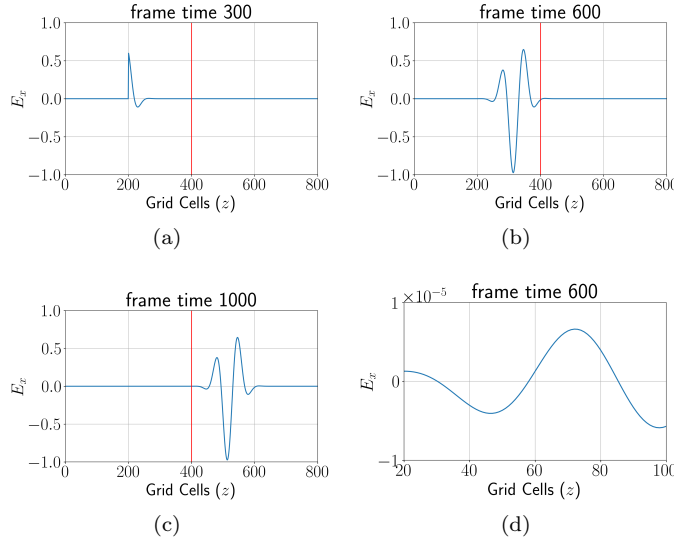


Figure 2. 2 fs pulse injected in 1D with absorbing boundary conditions with the addition of the total-field scattered-field approach. (a) - (c) show the pulse at sequential time-steps. (d) shows the grid “zoomed in” to view the amount of field which is still injected backward.

in Fig. 3. The interaction of the 1D E-field with the thin film is obvious and one can clearly make out the reduction in wavelength inside the dielectric. The TFSF approach also makes super clear, the amount of E-field which is a result of purely the reflected (or scattered) field due to the dielectric medium.

For reference, we have shown the transmission and reflection E-field amplitudes, along with the source amplitude as a function of time in the upper image in Fig. 4. The overall amplitude decreases as we might expect as the signal bounces between the walls of the thin film after entering. The expected periodicity in the transmission and reflection coefficients is also shown in the lower image in Fig. 4. Additionally, since we are not dealing with a lossy dielectric, we expect the sum of the transmission and reflection to add to one, which is also shown. We finally compared our numerical result, to the analytical expressions for the reflection and transmission coefficients and plotted the comparison in Fig. 5. We have ensured a value of points-per-wavelength of 25 at the injected pulse frequency (200 THz), however, for larger frequencies we will necessarily be plotting with less PPW. The accuracy of our numerical data is thus expected to worsen slightly for higher frequencies which is additionally shown in Fig. ??.

## B. Interaction with Lossy Media

As an extension of the results from the previous section, we decided to explore the interaction of a time-dependent injected pulse with a lossy medium. To do this, we considered two different frequency dependent dispersion models. The first was a Drude dispersion model which takes the form:

$$\epsilon_D(\omega) = 1 - \frac{\omega_p^2}{\omega^2 + i\omega\alpha}, \quad (2)$$

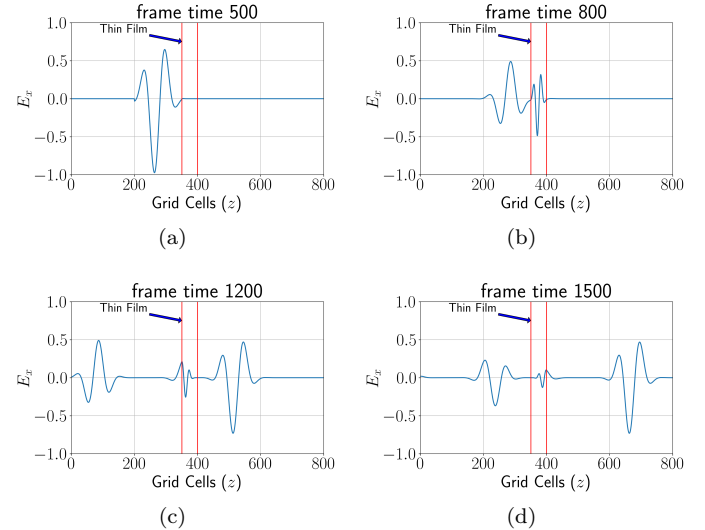


Figure 3. 2 fs pulse injected in 1D with same set-up as in Fig.’s 1 & 2. Dielectric thin film has a thickness of 1 micron with a dielectric constant of  $\epsilon = 9$ . Shown is a maximum of 1500 time-steps, though the simulation was run for 4000 steps of size  $dt$ .

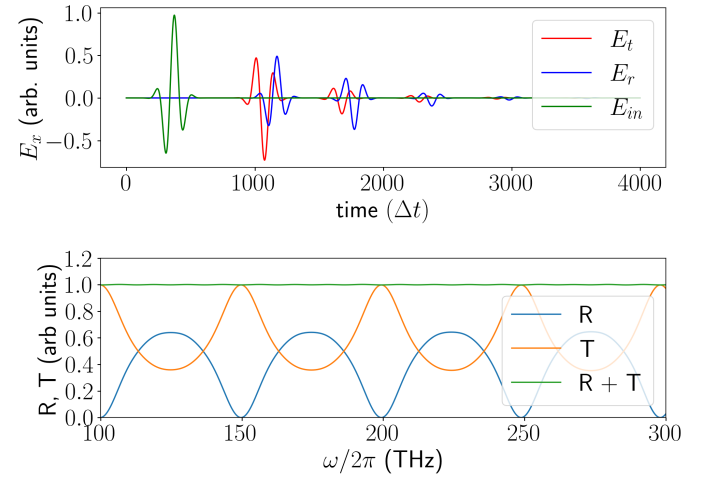


Figure 4. (Upper image) Transmitted, reflected, and injected (source) field amplitudes as a function of time. The source was injected at a position of 200 grid points,  $E_t$  is measured at 450 grid points, and  $E_r$  is measured at 100 grid points. (Lower image) Transmission and reflection coefficients as a function of frequency over a bandwidth which covers the injected pulse frequency (200-2 π THz).

where for our model, we used  $\alpha = 1.4 \times 10^{14}$  rads/s for the decay rate and  $\omega_p = 1.26 \times 10^{15}$  rads/s for the plasma frequency. The form of the frequency-dependent dispersion model above implies that we should see a change in the sum of the reflection and transmission coefficients depending on the frequency of the E-field. For a 1-fs pulse, with a center frequency of 200-THz, we simulated the E-field interaction with the Drude thin film with a thickness of both 200nm (Fig.s 6 & 7) and 800nm (Fig.’s 8 & 9).

Since it is now a lossy medium that we are considering, we can see that the sum of the transmission and reflection coefficients is no longer equal to one. In other words,

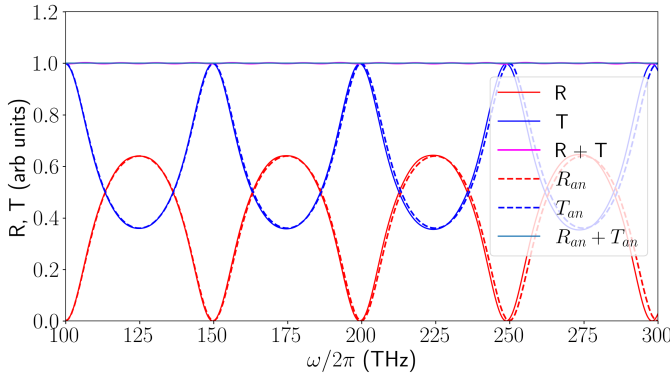


Figure 5. Numerical and analytical reflection and transmission coefficients over the same bandwidth shown in Fig. 4.

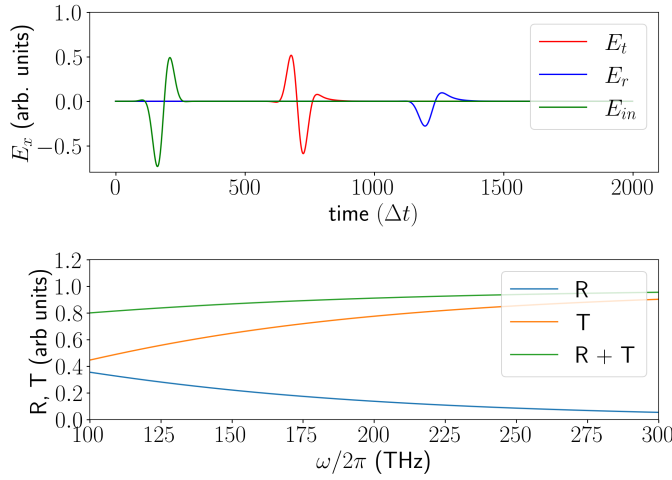


Figure 6. (Upper image) Transmitted, reflected, and injected (source) field amplitudes as a function of time. Corresponding to the Drude dispersion model for a thin film of thickness 200nm. (Lower image) Transmission and reflection coefficients as a function of frequency over a bandwidth which covers the injected pulse frequency ( $200 \cdot 2 \pi$  THz).

depending on the frequency, we sometimes achieve more or less reflection/transmission. The Drude model causes the thin film to act like a much “harder” medium which is why we only see one major pulse for the transmitted and reflected part of the signal.

The second dispersion model we considered was a Lorentz dispersion model, which takes the form:

$$\epsilon_L(\omega) = 1 + \frac{f_0 \omega_0^2}{\omega_0^2 \omega^2 - i 2 \omega \alpha}, \quad (3)$$

for which  $\alpha = 4\pi \times 10^{12}$  rads/s now and  $\omega_0 = 2\pi \cdot 200 \times 10^{12}$  rads/s is the resonant frequency of the oscillator. In analogy with the trials using the Drude model, we simulated the E-field interaction of a 1-fs time-dependent pulse interacting with both a 200nm (Fig.’s 10 & 11) and an 800nm (Fig.’s 12 & 13) thin film. Whereas for the Drude model, a total run time of 2000 time-steps allowed the system to come to rest, we required a much longer run time of  $\sim 6000$  time-steps to allow the ripples to go to zero for the case of the Lorentz dispersion model.

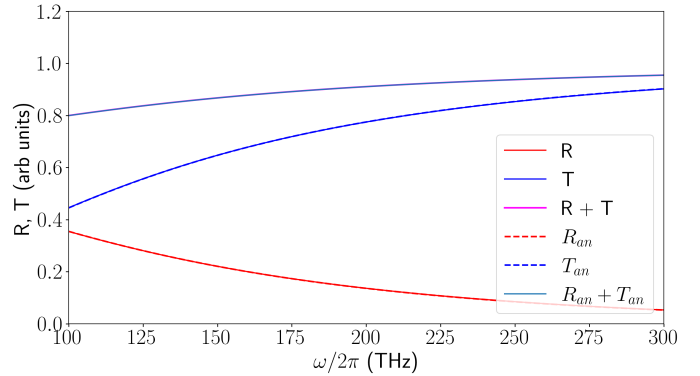


Figure 7. Numerical and analytical reflection and transmission coefficients for the same set-up as in Fig. 6

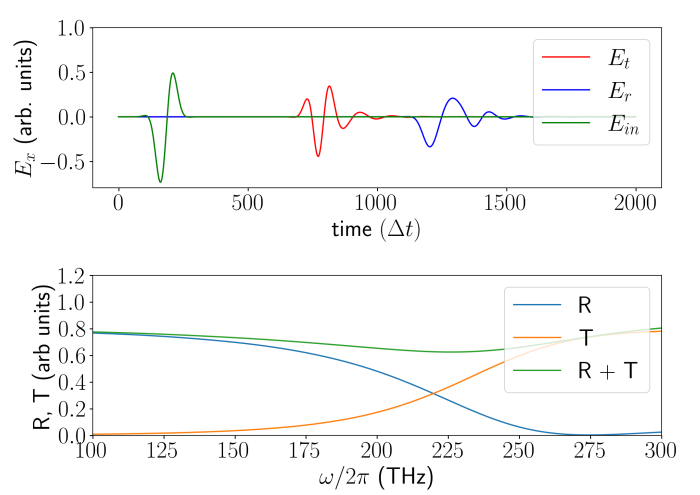


Figure 8. (Upper image) Transmitted, reflected, and injected (source) field amplitudes as a function of time. Corresponding to the Drude dispersion model for a thin film of thickness 800nm. (Lower image) Transmission and reflection coefficients as a function of frequency over a bandwidth which covers the injected pulse frequency ( $200 \cdot 2 \pi$  THz).

From the plots of the transmitted and reflected fields as a function of time, we can see that most of the initial pulse is let through the Lorentz medium, but with a number of trailing ripples. This effect is made more clear for the thicker thin film, indicating the longer the E-field propagates through the thin film, the more the initial pulse is damped. It is also clear from the frequency plots (Fig.’s 10(bottom) & 12(bottom)) in the Lorentz dispersion model, that the majority of the frequencies comprising the pulse are transmitted, while the center frequency is mostly reflected. Since the intensity of the pulse peaks at this frequency, we can see that the Lorentz model favours reflection at the frequency corresponding to the largest peak in intensity, while allowing all other frequencies through the medium more easily.

In both the Drude model and the Lorentz model, we have also compared our numerical FFT calculations to the analytical expressions for each model. These can be seen in Fig.’s 7, 9, 11, and 13, which show an almost perfect agreement between our numerical calculations and the expected

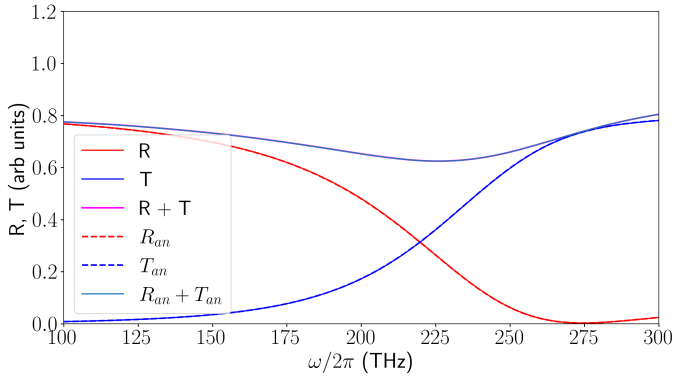


Figure 9. Numerical and analytical reflection and transmission coefficients for the same set-up as in Fig. 8

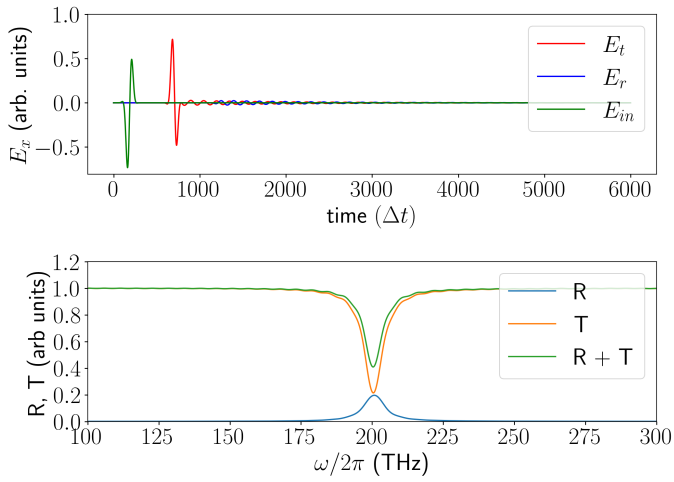


Figure 10. (Upper image) Transmitted, reflected, and injected (source) field amplitudes as a function of time. Corresponding to the Lorentz dispersion model for a thin film of thickness 200nm. (Lower image) Transmission and reflection coefficients as a function of frequency over a bandwidth which covers the injected pulse frequency ( $200 \cdot 2 \pi$  THz).

result.

### C. 2D FDTD and Speed-Up Techniques

Grid Size	BC (s)	N (s)	S (s)	N + S (s)
500x500	82.55	1.19	8.90	5.35
1000x1000	165.82	5.78	39.80	23.65

Table I. Run time comparison using the base code (BC), only using numba (N) as an optimization technique, only using array slicing (S) as the optimization technique, and using both numba and slicing (N + S) as the speed up technique.

Finally, we made the jump to two dimensions and examined the case of transverse magnetic (TM) modes on a two-dimensional (2D) grid. We began with a very simple non-optimized “base-code” that worked to produce images of the field intensity at various time-steps, in analogy to the field amplitudes in the 1D case. Similar to the 1D

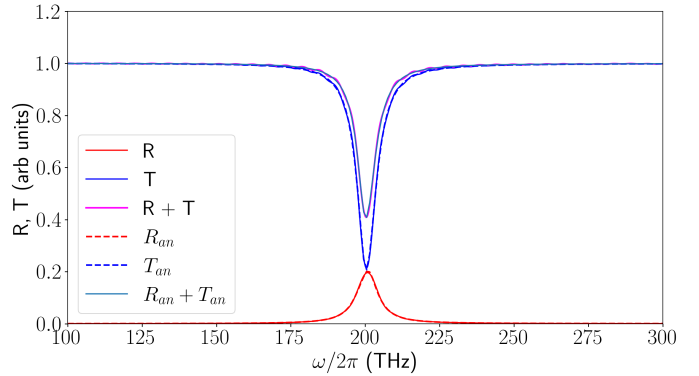


Figure 11. Numerical and analytical reflection and transmission coefficients for the same set-up as in Fig. 10

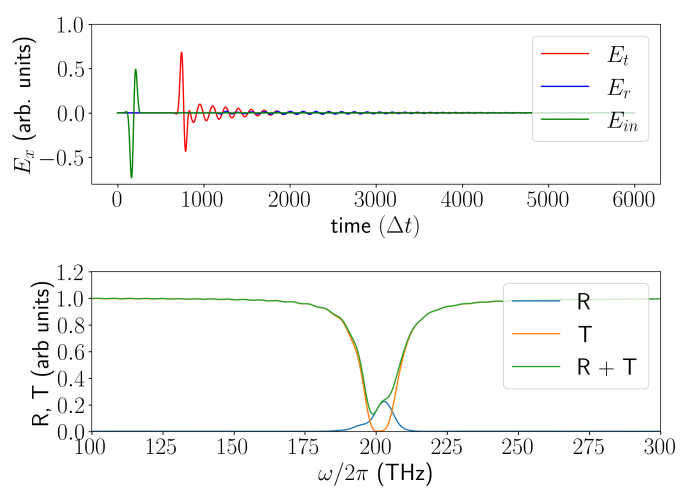


Figure 12. (Upper image) Transmitted, reflected, and injected (source) field amplitudes as a function of time. Corresponding to the Lorentz dispersion model for a thin film of thickness 800nm. (Lower image) Transmission and reflection coefficients as a function of frequency over a bandwidth which covers the injected pulse frequency ( $200 \cdot 2 \pi$  THz).

case, our 2D set-up used a time-dependent pulse, originating at a pre-determined location on the grid. For the more complex 2D case, we chose to stick to implementing a linear dielectric, though the implementation of a dispersion model would not differ greatly from that of the 1D case. In the case of 2D however, the dielectric material is of course a box and not simply a 1D film of a given thickness.

Using the non-optimized base-code, we began by simulating a 1-fs time-dependent pulse for a total of 1000 time-steps on a grid size of 160x160 grid points. We also chose to keep the grid spacing and time spacing the same as in the 1D examples so that  $dx$  and  $dt$  remained the same. As an initial example, we chose to vary the dielectric constant inside the box from  $\epsilon = 1$  (no dielectric) to  $\epsilon = 9$ . As a reference, we found our non-optimized code took roughly seconds without animation to compute the total number of time-steps for a grid size of 160x160. Some example plots showing the effect of increasing the dielectric constant are shown in Fig. 14 for the same time-step.

After viewing the solution for 1000 time-steps, we in-

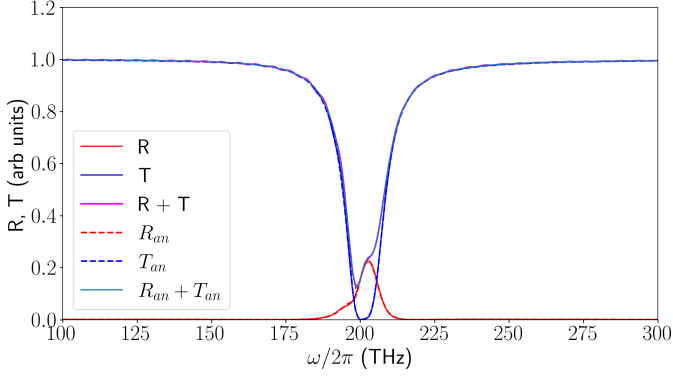


Figure 13. Numerical and analytical reflection and transmission coefficients for the same set-up as in Fig. 12

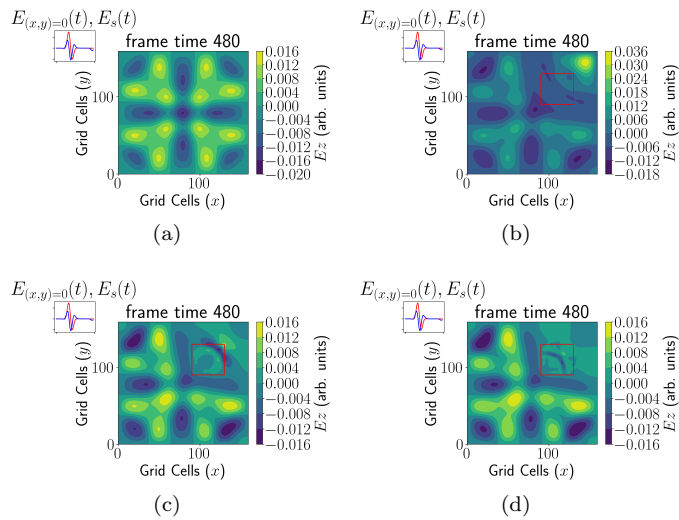


Figure 14. 2D example for a small grid size of 160x160. (a) - (d) show the same time step but an increasing dielectric constant in the box. Dielectric constants are 1, 3, 9, and 20 respectively. The E-field amplitude at the center of the grid and the source amplitude as a function of time are both shown in the smaller upper left plot of each main plot.

vestigated the effect of several speed up techniques and benchmarked each of them. We compared our completely non-optimized code to our code when using Numba, vectorization, and both Numba and vectorization. Our run times for a grid size of both 500x500 and 1000x1000 for 1000 time steps are shown in Table I. We found that using numba alone, resulted in at least an order of magnitude speed up, when compared to our base code. While array slicing implemented into our main routine sped things up considerably, numba was still far faster. Interestingly, we found that although both numba and slicing techniques sped up the code by a considerable margin when used alone, the use of these two techniques together, was slower than using numba alone, but faster than using vectorization alone.

As an attempt at further speeding up our computation time, we parallelized our code and ran it on CAC for 1, 2, 4, 8, and 16 processes and compared the speed up times. Our findings are summarized in Table II. For our run times for our parallel code, we used a grid size of 3008x3008 for a

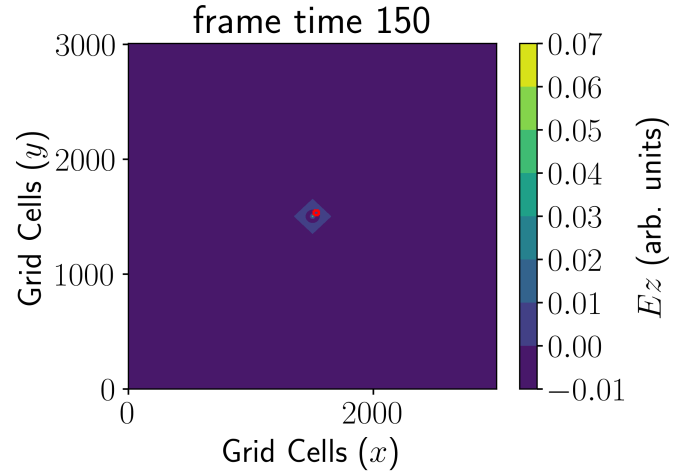


Figure 15. 2D FDTD simulation ran on the CAC for grid size of 3008x3008 for a total of 2600 time steps. Uses a value of 20 for the dielectric constant.

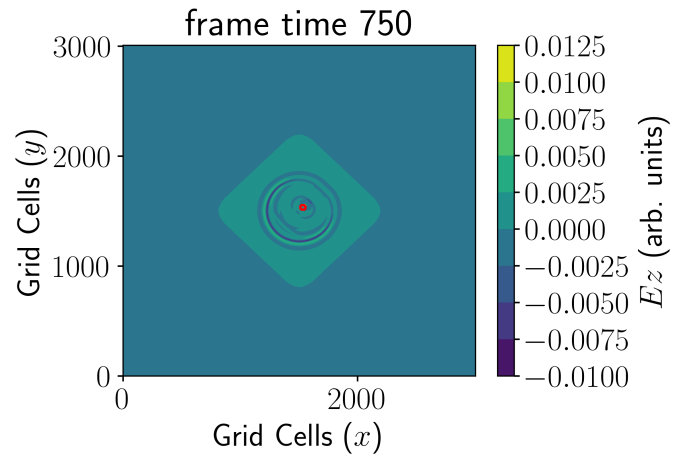


Figure 16. Same as in Fig. 15

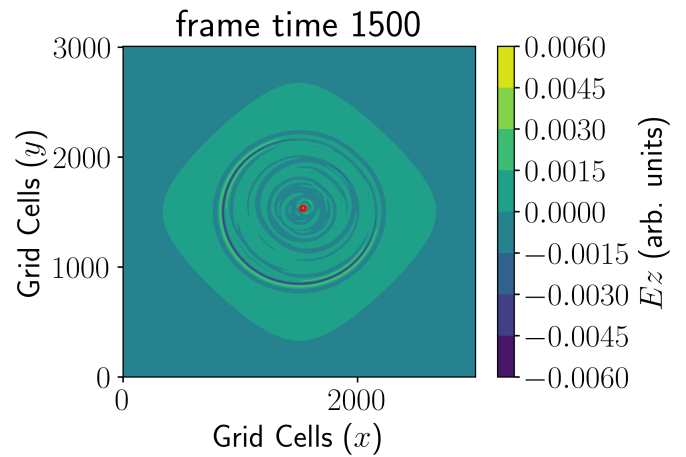


Figure 17. Same as in Fig. 15

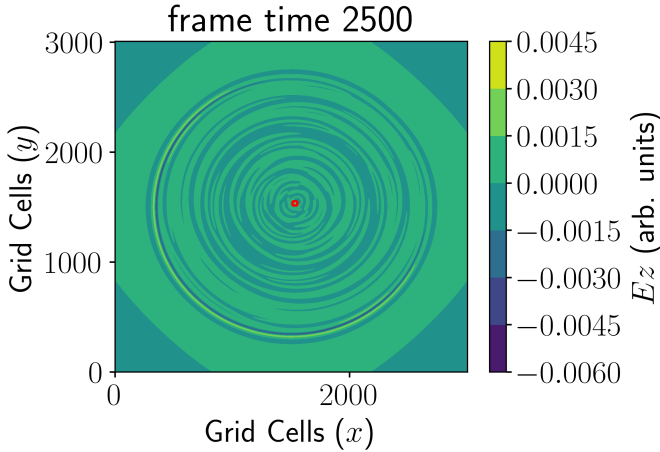


Figure 18. Same as in Fig. 15

ntasks	Pyth.	user	sys	user + sys	t/ntasks
1	309.12	242.679	68.791	311.47	311.47
2	151.80	246.04	61.348	307.388	153.694
4	66.69	271.604	1.101	272.705	68.18
8	37.83	311.266	2.187	313.453	39.18
16	25.80	428.44	4.771	433.211	27.08

Table II. Run time comparison for different number of processes using our parallel code and CAC. ntasks represents the number of processes used, Pyth. refers to the in-line python timer used across rank 0, user and sys are the user and system Linux times respectively, and t/ntasks is the sum of the sys + user time divided by the number of processes used in the computation. Each trial used 1 node and 1 cpu per task.

total of 1000 time steps. We found that indeed the amount of time per task was decreased by dividing up the work among several processes. Since running our code in parallel allowed for the use of a large grid, we used the CAC to produce the high quality, large grid images seen in Fig.'s 15, 16, 17, and 18. We simulated for a longer time of 2600 time steps to try and view the effect of the dielectric box ( $\epsilon_{box} = 20$ ) in this case on the larger grid.

#### Appendix A: E-field Plots for Dispersion Models

On the following page we show for reference, the E-field in space as it interacts with the thin film for each the Drude dispersion model and the Lorentz model. We show time stamps of our animation for each of the thin film thicknesses. These are 200nm and 800 nm.

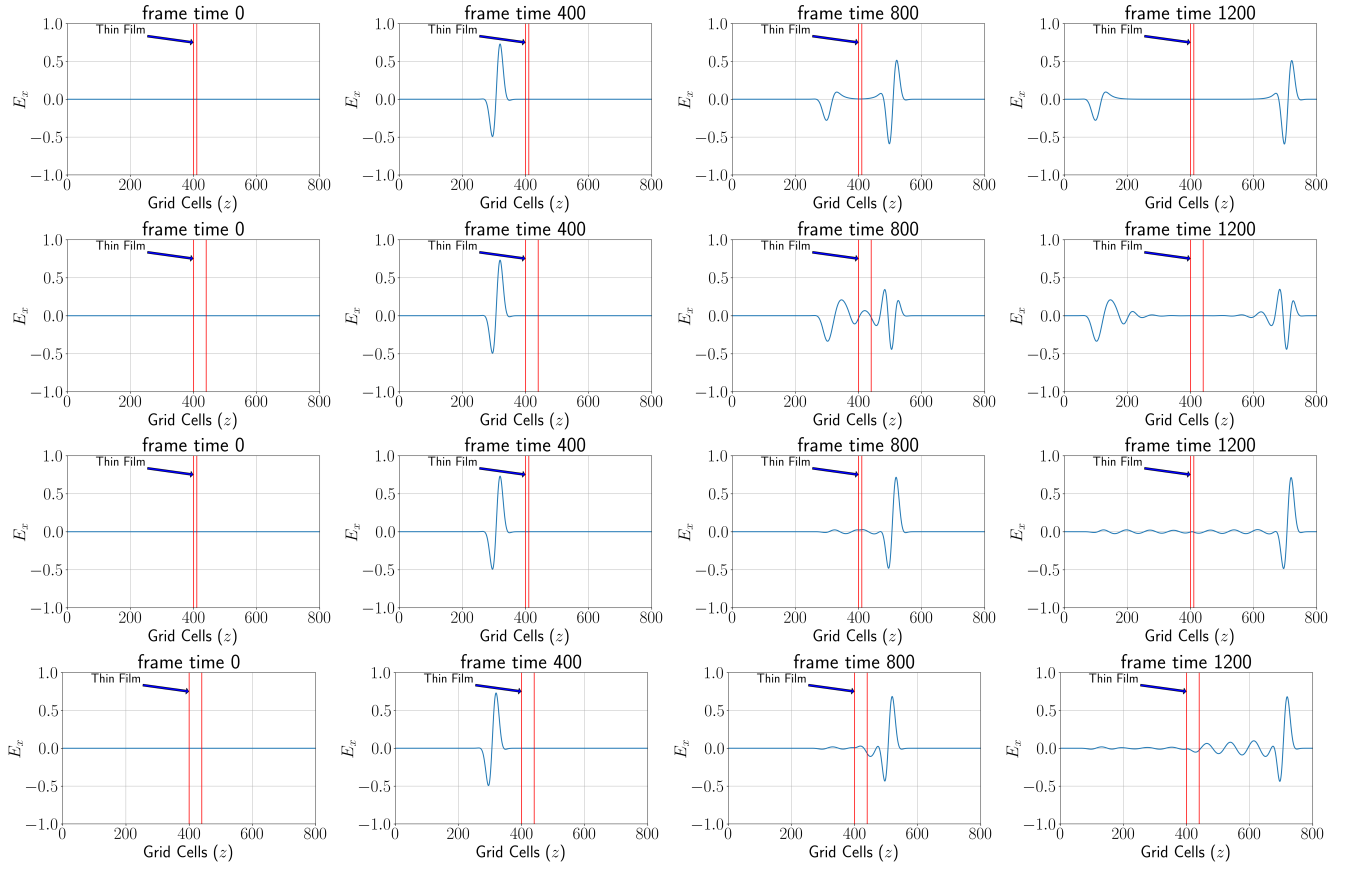


Figure 19. Electric field in space for the Drude (first two rows) and Lorentz (third and fourth) dispersion model. The first row uses a thin film with thickness equal to 200nm. The second row show the interaction for a thin film with thickness 800nm. The third row similarly shows a 200nm film with the fourth showing interactions with an 800 nm film.